SPATIAL NORMALISATION OF THREE-DIMENSIONAL NEUROANATOMICAL MODELS USING SHAPE REGISTRATION, AVERAGING, AND WARPING

Philippe ANDREY[1,2]*, Emeric MASCHINO*[1]*, and Yves MAURIN*[1]

[1]Analyse et Modélisation en Imagerie Biologique, Laboratoire de Neurobiologie de l'Olfaction et de la Prise Alimentaire, INRA UMR 1197, Jouy-en-Josas, France
[2]Université Pierre et Marie Curie, Paris, France

ABSTRACT

In neuroanatomical studies, the specimens are generally cut into serial sections that are processed to reveal the elements of interest. The third dimension lost during sectioning can be recovered by reconstructing three-dimensional graphical models of the studied structures. To reach statistical significance and to compare results from distinct experiments, data from different models must be combined into common representations. Due to biological and experimental variability, this requires a non-linear spatial normalisation step. In this paper, an algorithm is presented to normalise and map data into average models. The usefulness of the approach for elucidating spatial organisations in the nervous system is illustrated on rat neuroanatomical data.

***Index Terms*—** Neuroanatomy, 3D reconstruction, modelling, spatial organisation, rat nervous system.

1. INTRODUCTION

The activity of the nervous system is ensured by neuronal populations that are organised in three dimensions. Three-dimensional (3D) representations of neuroanatomical organisations are thus essential to the study and understanding of brain function. A number of techniques, such as confocal microscopy and magnetic resonance microscopy, are available to image brain structures of small laboratory animals. However, conventional histological microscopy remains the methodology of choice to study the organisation of neuronal structures with a tissular resolution over wide observation fields. Hence, neuroanatomical studies typically consist in revealing and mapping specific neuronal markers on two-dimensional (2D) serial sections. The third dimension lost by sectioning the specimen can be recovered using 3D reconstruction from stacked serial sections. This generates graphical models of the studied structures that can be interactively explored and quantitatively analysed.

Each 3D model is generated from data collected during a single experiment on a single animal. The variability is not accounted for in such an individual model. Besides, the number of structures that can be simultaneously revealed on a given animal is limited in practice. Studying a complex neuroanatomical ensemble therefore encompasses a series of distinct experiments. This yields a collection of individual models, providing each an incomplete view of the studied organisation. Generating statistically representative and anatomically comprehensive 3D models requires that data from individual models be combined. Large morphological fluctuations are observed in practice among 3D models, if only because of the physical and chemical alterations due to histological processing. Hence, data integration from different models should incorporate a spatial normalisation step.

Spatial normalisation of 3D images has received considerable attention, in particular in non-invasive brain imaging. Surprinsingly, very few studies have addressed the problem of normalising data from serial section reconstructed models. Funka-Lea and Schwaber [4] proposed an interactive method for locating and warping data from a 2D section onto a 3D atlas. Recently, methods have been proposed to combine 3D models normalised for position, orientation, and scale [3, 5, 8]. These affine methods do not compensate for 3D shape fluctuations. In [2], we have introduced a method based on coarse model alignment and polynomial warping. This method achieves a non-linear normalisation, which is mandatory to rectify the morphological fluctuations due to biological and experimental variability. However, it may fail to correctly normalise models in some situations because of the absence of a true registration step.

This paper presents an improved method to combine data from individual 3D models built from serial sections. Our original method has been improved by incorporating a true surface registration and averaging algorithm [6]. The method relies upon the existence of reference structures, i.e., structures whose instances are homologous across models. The morphological variations of the references around their averages are assumed representative of the deformations affecting the whole specimen. Under this assumption, normalisation is achieved by registering and averaging the references, modelling the deformations around their averages, and warping the other structures by propagating these deformations. The method is detailed in Section 2. Sample results obtained on

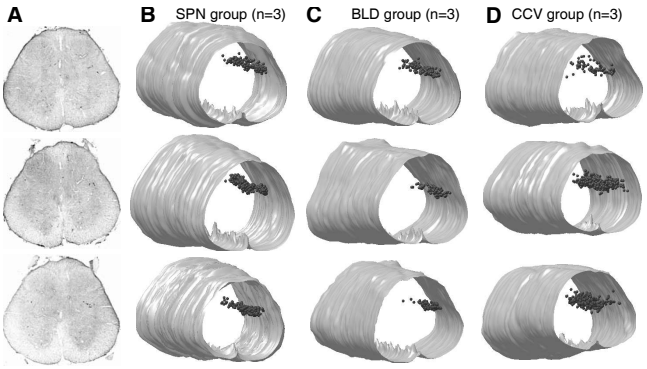

Fig. 1. 3D reconstruction and modelling of the SPN. (A) Sample coronal sections. (B) Models of the whole SPN population. (C) Models of the subpopulation innervating the bladder. (D) Models of the subpopulation innervating the penis. Grey matter boundary and central canal were omitted for clarity.

rat neuroanatomical data are reported and briefly discussed in Section 3. Section 4 concludes the paper.

2. MATERIAL AND METHODS

2.1. Neuroanatomical data

The data were collected in a study of the spatial organisation of the rat sacral parasympathetic nucleus (SPN) [2]. The SPN, located in the lumbo-sacral segments of the spinal cord, contains neuronal populations that control the reflex motricity of uro-genital organs. The study aimed at determining whether SPN populations controlling different organs are spatially segregated or not. To this end, SPN cells were labelled using retrograde neuronal tracers. In a first group of three rats (SPN group), samples of the whole SPN population were labelled. In three other rats (BLD group), only cells innervating the dome of the bladder were labelled. In yet three other rats (CCV group), only cells innervating the corpus cavernosum of the penis were labelled. In each case, the lumbo-sacral spinal cord was dissected out and serially cut into coronal sections (Fig. 1A). Care was taken to process homologous spinal cord segments in all nine animals.

2.2. Three-dimensional reconstruction and modelling

Three-dimensional reconstruction was performed using the *Free-D* software [1]. On each slice image, the contours of the spinal cord, of the grey/white matter boundary and of the central canal were delineated and the labelled cells were pointed. Following image registration, anatomical envelopes were reconstructed as quadrangular meshes from contour stacks using contour resampling, matching, and interpolation [6]. Any surface $\mathbf{S}$ was thus divided into quadrangles, its vertices being indexed on a $W \times H$ grid: $\mathbf{S} = \{\mathbf{p}(u,v) = [x(u,v), y(u,v), z(u,v)]^t : 0 \leq u < W, 0 \leq v < H\}$, H being the number of contours and W the number of vertices per contour. W and H were adjusted to keep reconstruction error, measured using the distance between original contour stacks and reconstructed surfaces, below a threshold. Due to shape differences, different mesh sizes were thus selected for the spinal cord (165×110), the grey/white matter boundary (175×110) and the central canal (10×110). For each structure, the same size was used in all animals. Figures 1B–D display the nine reconstructed models.

2.3. Model registration and surface averaging

To compute the average reference structures, the individual models must be registered. In most experimental conditions, the structures of interest are not the anatomical references and their spatial organisation is unknown. Consequently, model registration should be driven by references only while other structures should passively follow the transformations. In the present study, the spinal cord envelope, the grey/white matter boundary, and the central canal are the reference structures.

Models are first centered at the origin of the coordinate frame and coarsely oriented by aligning the principal axes of their references with those of the coordinate frame. If several reference structures are present in each model, they are processed as a single, multi-parts object. The translation and rotation are computed using references only, but are applied to non-reference model components as well.

The principal axes transformation independently aligns each model with the main coordinate frame. It does not guarantee the minimisation of residual distances among all references. Therefore, this initial, coarse alignment is refined using a multiple surface registration algorithm [6]. For the sake of completeness, this algorithm is briefly summarised below.

The algorithm iteratively registers each model onto the average of the other ones. Let N denote the number of individual models, K the number of references in each model, M_i the ith model and $\mathbf{S}_i^{(k)}$ the kth reference in M_i. During an iteration, each model M_i is considered in turn. First, a partial average model $\bar{M}_i$ is built with the remaining ones. $\bar{M}_i$ contains K average references $\bar{\mathbf{S}}_i^{(k)}$ defined by:

$$\bar{\mathbf{S}}_i^{(k)}(u,v) = \frac{1}{N-1} \sum_{j \neq i} \mathbf{S}_j^{(k)}(u,v) \qquad (1)$$

Each $\mathbf{S}_i^{(k)} (1 \leq k \leq K)$ is then reparameterised to ensure that vertex numbering is anatomically coherent with $\bar{\mathbf{S}}_i^{(k)}$. This matching consists in minimising the sum of squared vertex-to-vertex distances between $\mathbf{S}_i^{(k)}$ and $\bar{\mathbf{S}}_i^{(k)}$ over all u-index circular permutations (v-index correspondence results from contour stacking). Model M_i is then registered on $\bar{M}_i$ by applying rotation $\hat{\mathbf{R}}$ and translation $\hat{\mathbf{t}}$ that minimise the quantity:

$$\sum_{k=1}^{K} \sum_{u=0}^{W-1} \sum_{v=0}^{H-1} \|\mathbf{R}\mathbf{S}_i^{(k)}(u,v) + \mathbf{t} - \bar{\mathbf{S}}_i^{(k)}(u,v)\|^2 \qquad (2)$$

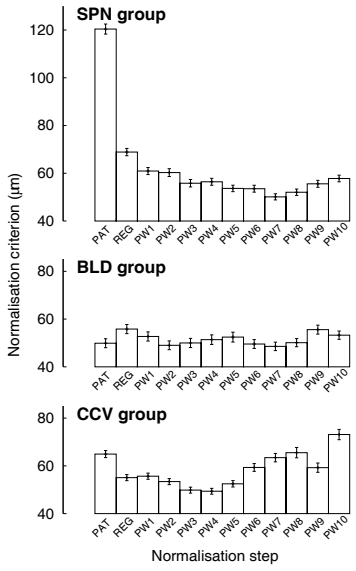

Fig. 2. Evolution of the criterion during normalisation. The criterion was computed after principal axes alignment (PAT), model registration (REG), and warping (PW). In the latter case, the number indicates the degree D of the polynomials.

$\hat{\mathbf{R}}$ and $\hat{\mathbf{t}}$ are computed using a singular value decomposition approach [7]. Note that a single rotation and translation are determined and applied to all the components of M_i.

The algorithm generally converges within a few iterations. The final, resulting average model $\bar{M}$ is computed by averaging the references over the N individual, registered models.

At the end of the surface reconstruction process (Sect. 2.2), the vertices of $\mathbf{S}_2^{(k)}, \ldots, \mathbf{S}_N^{(k)}$ are generally not in anatomical correspondence. An initialisation step is thus required to ensure the anatomical validity of the model $\bar{M}_1$ computed in the first iteration. To this end, $\mathbf{S}_3^{(k)}$ to $\mathbf{S}_N^{(k)}$ are reparameterised to match $\mathbf{S}_2^{(k)}$ before entering the algorithm main loop.

2.4. Individual models warping and merging

Model warping consists in considering each individual model in turn and in mapping its non-reference components into the average model using non-linear deformations. To this end, a parametric deformation model is adopted and fitted to the observed displacements that map the reference structures onto their averages. The deformation model can then be applied to evaluate the deformation at any position in the 3D space.

The discrete deformation field $\mathbf{d}_i^{(k)}$ that maps any reference $\mathbf{S}_i^{(k)}$ of model M_i onto its average in $\bar{M}$ is given by:

$$\mathbf{d}_i^{(k)}(u,v) = \bar{\mathbf{S}}^{(k)}(u,v) - \mathbf{S}_i^{(k)}(u,v) \tag{3}$$

Fitting a parametric deformation model to these data can be achieved using either interpolation or approximation. Surfaces reconstructed from physical serial sections are affected by cumulated errors from histological processing, registration, and segmentation. The sample deformation fields between references and their averages thus contain large numbers of noisy data. In this context, deformations should be approximated rather than interpolated.

A multivariate polynomial approximation scheme is adopted here. Any position $\mathbf{p}$ is mapped to $\mathbf{p}' = \mathbf{p} + \boldsymbol{\delta}(\mathbf{p})$, where $\boldsymbol{\delta} = (\delta_X, \delta_Y, \delta_Z)$ is a vector of three trivariate polynomials of arbitrary degree D. For example:

$$\delta_X(x,y,z) = \sum_{a+b+c \leq D} \alpha_{abc}\ x^a y^b z^c \tag{4}$$

The polynomial coefficients $\{\alpha_{abc}\}$ are determined using least-squares estimation, i.e., by minimising the quantity:

$$\sum_{k=1}^{K} \sum_{u=0}^{W-1} \sum_{v=0}^{H-1} \|\boldsymbol{\delta}(\mathbf{S}_i^{(k)}(u,v)) - \mathbf{d}^{(k)}(u,v)\|^2 \tag{5}$$

To this end, an orthogonal polynomial decomposition is used. Our implementation is based on a generalisation of Horner's scheme to multivariate polynomials. It can represent polynomials with any number of variables up to any degree. This facilitates investigations in order to find the best polynomial order to model morphological variations.

2.5. Quantitative evaluation of spatial normalisation

The polynomial deformation order D is the main free parameter of our spatial normalisation method. Setting D by visually examining normalised models is not only subjective, but also often impossible because of the difficulty of comparing 3D graphical representations. Therefore, an objective criterion is introduced to quantitatively evaluate normalisation results.

The normalisation criterion is defined in the context of repeated experiments. It quantifies the spatial coherence of the n point sets that result from labelling a given neuronal population on n animals. It is assumed that, since the point sets are samples of the same population, they should be brought into correspondence by normalisation. For each cell of each set, the distance to the nearest cell among the $n-1$ other sets is computed. The criterion is the average of all these distances. Low values indicate good spatial coherence. The optimal D value is thus found by minimising the normalisation criterion.

3. RESULTS AND DISCUSSION

Following alignment, the nine individual models were registered (10 iterations) and warped using polynomial deformations of degree D varying from 1 to 10. Within each experimental group, the normalisation criterion was computed at each step of the process (Fig. 2). The minimum was reached for degree 4 within the CCV group and degree 7 for the SPN

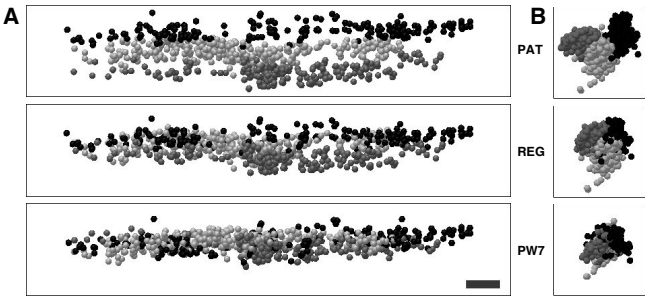

Fig. 3. The three sets of cells (represented with different grey levels) in the SPN group after alignment (PAT), registration (REG), and warping of degree 7 (PW7). Views are (A) sagittal and (B) coronal. Scale bar: 250 μm.

and BLD groups. In both SPN and CCV groups, the evolution of the criterion presented a clear minimum. The value at the minimum was remarkably similar in the three groups. This suggests that an absolute minimum has probably been reached. The pattern within the BLD group was more or less flat. Within this group, it appears that the three point sets were already in good correspondence after the initial alignment.

The evolution of the spatial relationships between the three point sets of the SPN group is displayed Figure 3. The large misregistration that subsists after initial alignment is reduced by the global model registration step. This illustrates the improvment gained by adding the registration step, which was absent in our first normalisation method [2]. However, a good correspondence is only obtained by applying the optimal polynomial warping (degree 7). This confirms that linear or affine correction methods are not sufficient to rectify the morphological variations that affect our models.

The superposition of the normalised cell populations of the BLD and CCV groups is shown within the average spinal cord envelope in Figure 4. In the coronal plane, the two subpopulations are in good correspondence. Conversely, they occupy different territories in the parasagittal plane. Cells innervating the penis are located in the rostral end of the lumbosacral spinal cord, while cells innervating the bladder are located at the caudal end. Lastly, the segregation is only partial since the two subpopulations overlap in the middle part of the considered spinal cord region. These results confirm that the BLD and the CCV subpopulations of the SPN are partially segregated along the rostro-caudal direction [2].

4. CONCLUSION

The proposed algorithm allows the spatial normalisation of 3D neuroanatomical models built from serial sections. It takes into account the non-linear morphological variations of the individual models, a prerequisite for integrating data from different individuals and experiments into common, average representations. Since it smoothes out individual variability, this

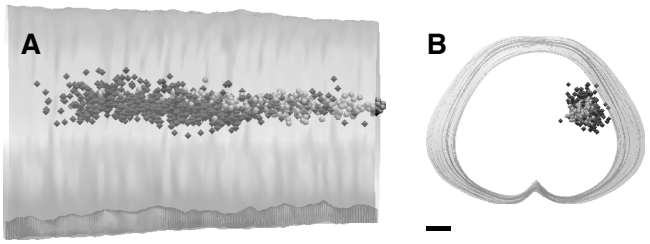

Fig. 4. Superposition of the three BLD (spheres) and the three CCV (diamonds) subpopulations following spatial normalisation. Views are (A) sagittal; (B) coronal. Scale bar: 250 μm.

methodology should help to decipher the complex architectural rules that govern the organisation of the nervous system.

5. REFERENCES

[1] P. Andrey and Y. Maurin. *Free-D*: an integrated environment for three-dimensional reconstruction from serial sections. *J. Neurosci. Methods*, 145(1–2):233–244, 2005.

[2] B. Banrezes, P. Andrey, E. Maschino, A. Schirar, J. Peytevin, O. Rampin, and Y. Maurin. Spatial segregation within the sacral parasympathetic nucleus of neurons innervating the bladder or the penis of the rat as revealed by three-dimensional reconstruction. *Neurosci.*, 115(1):97–109, 2002.

[3] A. Brevik, T. B. Leergaard, M. Svanevik, and J. G. Bjaalie. Three-dimensional computerised atlas of the rat brain stem precerebellar system: approaches for mapping, visualization, and comparison of spatial distribution data. *Anat. Embryol.*, 204(4):319–332, 2001.

[4] G. D. Funka-Lea and J. S. Schwaber. A digital brain atlas and its application to the visceral neuraxis. *J. Neurosci. Methods*, 54(2):253–260, 1994.

[5] P. Mailly, S. Charpier, A. Menetrey, and J.-M. Deniau. Three-dimensional organization of the recurrent axon collateral network of the subtantia nigra pars reticulata neurons in the rat. *J. Neurosci.*, 23(12):5247–5257, 2003.

[6] E. Maschino, Y. Maurin, and P. Andrey. Joint registration and averaging of multiple 3D anatomical surface models. *Comput. Vis. Image Underst.*, 101(1):16–30, 2006.

[7] S. Umeyama. Least-squares estimation of transformation parameters between two point patterns. *IEEE Trans. Patt. Anal. Mach. Intell.*, 13(4):376–380, 1991.

[8] L. Zaborszky, D. L. Buhl, S. Pobalashingham, J. G. Bjaalie, and Z. Nadasdy. Three-dimensional chemoarchitecture of the basal forebrain: spatially specific association of cholinergic and calcium binding protein-containing neurons. *Neurosci.*, 136(3):697–713, 2005.